IOP Conference Series: Materials Science and Engineering

PAPER • OPEN ACCESS

Advanced Micromorphology Analysis of Cu/Fe NPs Thin Films

To cite this article: lu *et al* 2019 *IOP Conf. Ser.: Mater. Sci. Eng.* **611** 012016

View the article online for updates and enhancements.

This content was downloaded from IP address 41.89.227.170 on 15/05/2020 at 11:41

IOP Conf. Series: Materials Science and Engineering **611** (2019) 012016 doi:10.1088/1757-899X/611/1/012016

Advanced Micromorphology Analysis of Cu/Fe NPs Thin Films

Ş Ţălu[1,*], A Ghaderi[2], K Stępień[3] and F M Mwema[4]

[1]The Directorate of Research, Development and Innovation Management (DMCDI), The Technical University of Cluj-Napoca, Constantin Daicoviciu Street, no. 15, Cluj-Napoca, 400020, Cluj county, Romania
[2]Young Researchers and Elite Club, West Tehran Branch, Islamic Azad University, Tehran, Iran
[3]Faculty of Mechatronics and Mechanical Engineering, Kielce University of Technology, Al. 1000-lecia P. P. 7, 25-314 Kielce, Poland
[4]Department of Mechanical Engineering Science, University of Johannesburg, Auckland Park Campus, South Africa

*Corresponding author

Abstract. In this work, an advanced analysis of Cu/Fe NPs thin films using atomic force microscopy (AFM) has been discussed to characterize at nanoscale 3-D surface microtexture. Samples of Cu/Fe thin films were fabricated by Direct Current-Magnetron Sputtering technique with two controlled thicknesses (group I: Cu 55 nm/Fe 55 nm and group II: Cu 55 nm/Fe 70 nm) in specific conditions of pressure and power. The results obtained from experimental measurements suggested that the surface of group I has the lowest values for fractal dimension (D = 2.28 ± 0.01) and root mean square height (Sq = 4.40 ± 0.1 nm); while the highest values for fractal dimension (D = 2.31 ± 0.01) and root mean square height (Sq = 4.67 ± 0.1 nm) were found in group II. Stereometric and fractal analyses applied for thin films are modern tools for accurate quantitative morphometric characterisation.

1. Introduction

Nanoparticles (NPs) are defined as a various class of materials including a variety of particulate substances that have in at one external dimension approximately 1 to 100 nm [1, 2].
Metal nanoparticles can be considered a research field in full expansion with many industrial applications (automotive, electronic, petrochemical, chemical, military, aerospace, power generation, solar electric power, energy) due to their wide range of tunable physicochemical characteristics [3-5].
In recent decades, different types of Metal NPs have been reported and classified in various research reports depending on their chemical composition and crystalline forms [1]. In different studies about thin films prepared by various techniques of DC magnetron sputtering were applied different mathematical methods for evaluation of micro-roughness parameters [6-10].
Scientific reports with computerized procedures and interpretation in detail regarding the stereometric analysis of Cu/Fe NPs thin films and optimal research techniques for description of 3-D surface micromorphology are recorded in the scientific literature [3-5]. Furthermore, recent studies confirmed the 3-D (three dimensional) surface microtexture of thin films could be estimated using fractal [11-14] and multifractal [9, 15-18] analyses, as well as by power spectral density (PSD) functions [6, 19-21]. Also, it can be noted that microroughness of a surface texture obtained by AFM is usually considered in analyses only along z-axis (vertical axis) in correlation with measurement factors [22-25], while PSD analysis give information about lateral and vertical signals obtained from AFM micrographs [21,

Content from this work may be used under the terms of the Creative Commons Attribution 3.0 licence. Any further distribution of this work must maintain attribution to the author(s) and the title of the work, journal citation and DOI.
Published under licence by IOP Publishing Ltd

26-32]. In this work, the stereometric and fractal analysis, as well as PSD functions are applied to characterize different surface microtextures of samples (Cu/Fe NPs thin films) prepared by DC Magnetron sputtering technique considering AFM micrographs and the corresponding parameters, computed according with the standard ISO 25178-2:2012.

2. Materials and Methods

The experimental procedure to obtain samples with two controlled thicknesses (group I: Cu 55 nm/Fe 55 nm and group II: Cu 55 nm/Fe 70 nm) by DC Magnetron sputtering technique, in specific conditions of pressure (basic pressure, 10.7×10^{-3} Pa; work pressure 8 Pa) and power (20 Watt) has been published in details in our previous works [3-5].
Atomic force microscopy imaging was performed using a commercial Nanoscope Multimode AFM system (Digital Instruments, Santa Barbara, CA). The surfaces were scanned in non contact mode at a scan rate of 10–20 μm/s to record AFM images of 256 x 256 pixels for areas of 1 μm x 1 μm.

3. Results and Discussion

The stereometric, fractal and PSD analyses applied for AFM data were described in chosen terms of stereometric analysis using the MountainsMap Premium software version 7.4.8872 [33] and were calculated based on the definitions given in the standard ISO 25178-2:2012 [34].
The relevant AFM micrographs of the samples, for 1 μm x 1 μm scanning square areas, are illustrated in fig. 1.

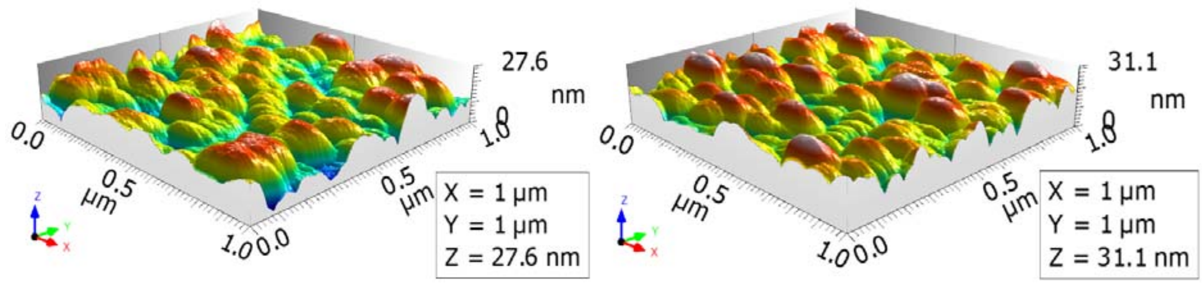

Figure 1. 3-D AFM micrographs of samples: a) group I; b) group II.

The root mean square height for group I is Sq = 4.40 [nm] and for group II is Sq = 4.67 [nm], whilst arithmetical mean height for group I is Sa = 3.58 [nm] and for group II is Sa = 3.79 [nm]. Also, the maximum height for group I is Sz = 27.6 [nm] and for group II is Sz = 31.1 [nm].
The representation of surface texture directions of analyzed samples using Cartesian graphs are shown in figure 2 and the corresponding values are given in Table 1.

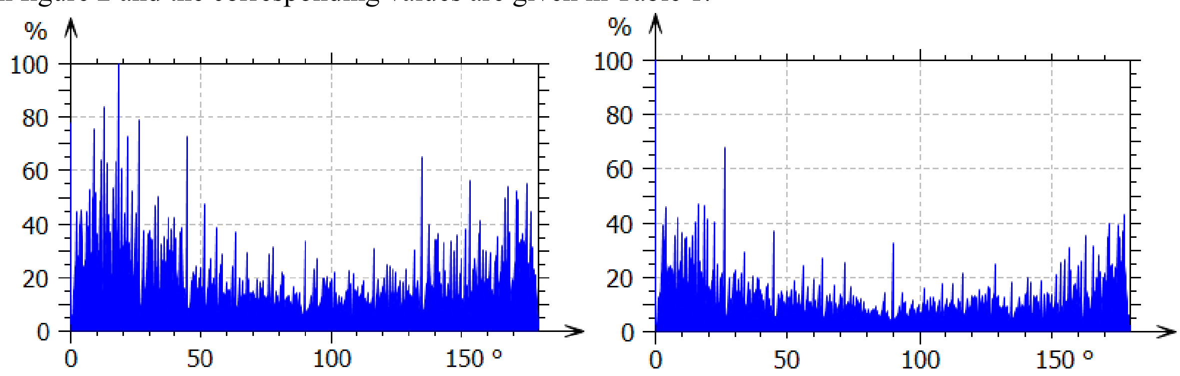

Figure 2. The representation of surface texture directions of analyzed samples using Cartesian graphs for: a) group I; b) group II.

Table 1. Surface texture directions of analyzed samples using Cartesian graphs.

Samples	Isotropy [%]	First direction [°]	Second direction [°]	Third direction [°]
Group I	60.8	18.5	13.0	26.5
Group II	49.5	0.10	26.5	16.0

The graphical representation of surface texture isotropy of analyzed samples using the autocorrelation functions are presented in figure 3.

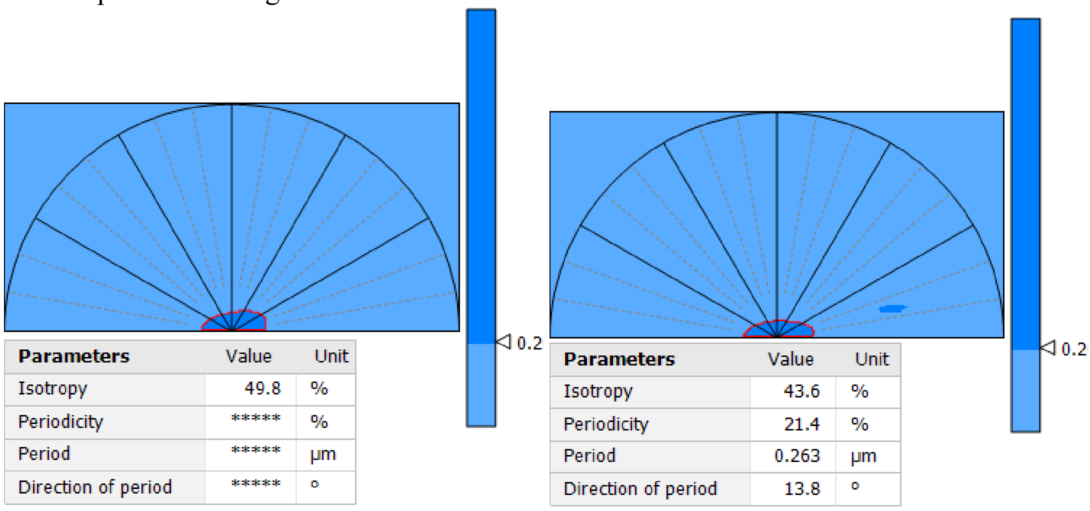

a) b)

Figure 3. The representation of surface texture isotropy of analyzed samples for: a) group I; b) group II.

Graphical representations of the furrows of the analyzed samples are illustrated in figure 4.

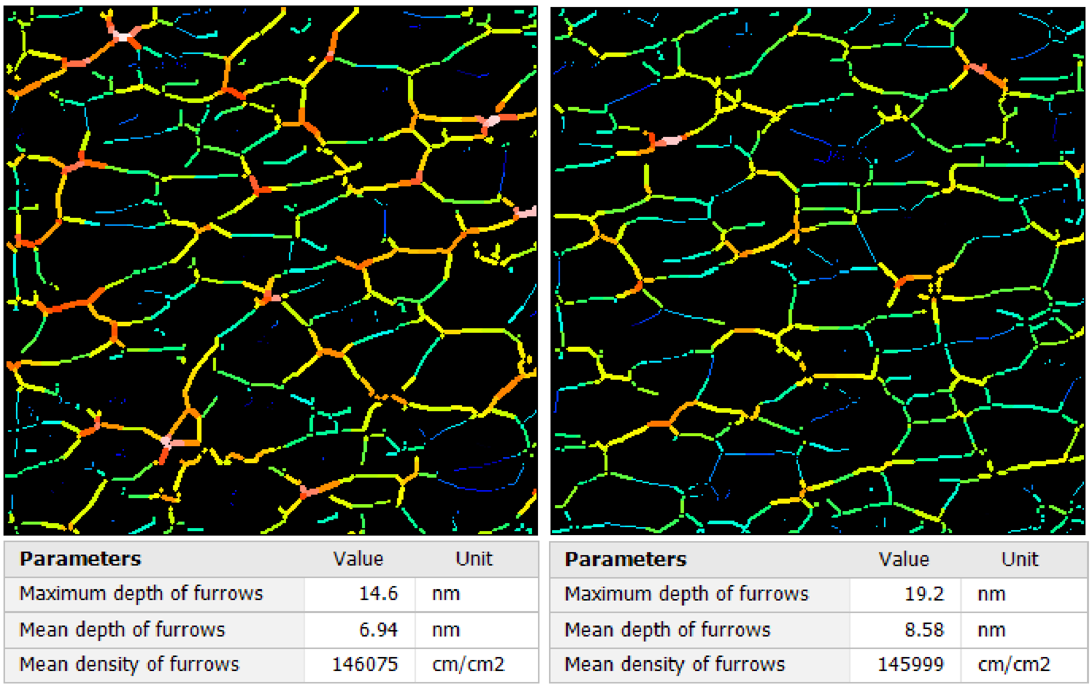

a) b)

Figure 4. The representation of the furrows for: a) group I; b) group II.

The values of the maximum depth of furrows and mean depth of furrows parameters are greater for group II, whereas the greater value of mean density of furrows is associated with group I.

Computation of the fractal dimension (Df) based on the enclosing boxes method [33] with determination of coefficients of correlation (R^2), are detailed shown in fig. 5.

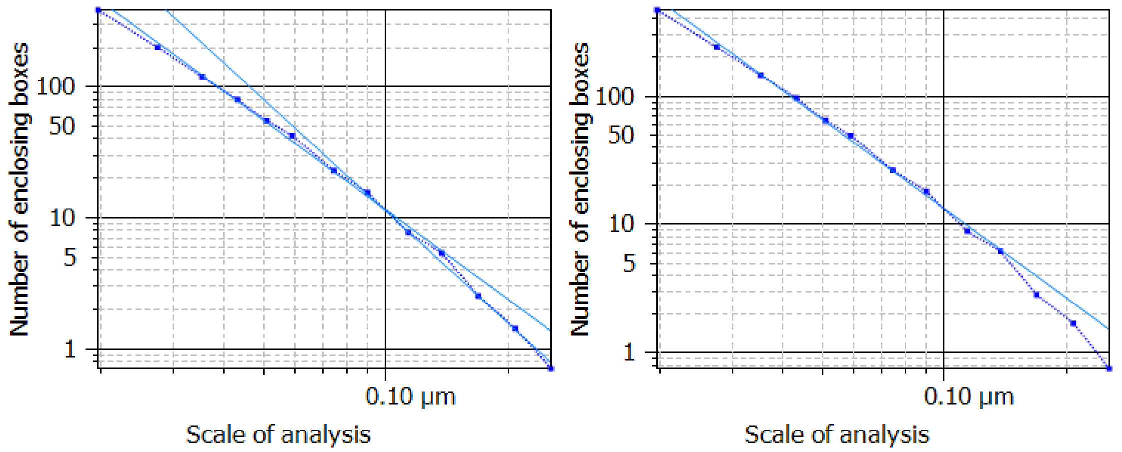

Information	
Method	Enclosing boxes

Parameters	Value
Fractal dimension	2.28
Slope(1)	-2.28
R²(1)	0.997
Slope(2)	-2.84
R²(2)	0.994

a)

Information	
Method	Enclosing boxe

Parameters	Value
Fractal dimension	2.31
Slope(1)	-2.31
R²(1)	0.997
Slope(2)	-2.61
R²(2)	0.993

b)

Figure 5. Graphs of the fractal dimension with coefficients of correlation (R^2), computed by the enclosing boxes method for: a) group I; b) group II.

The representation of averaged power spectrum density (PSD) of surface textures is shown in figure 6 with the corresponding parameter values.

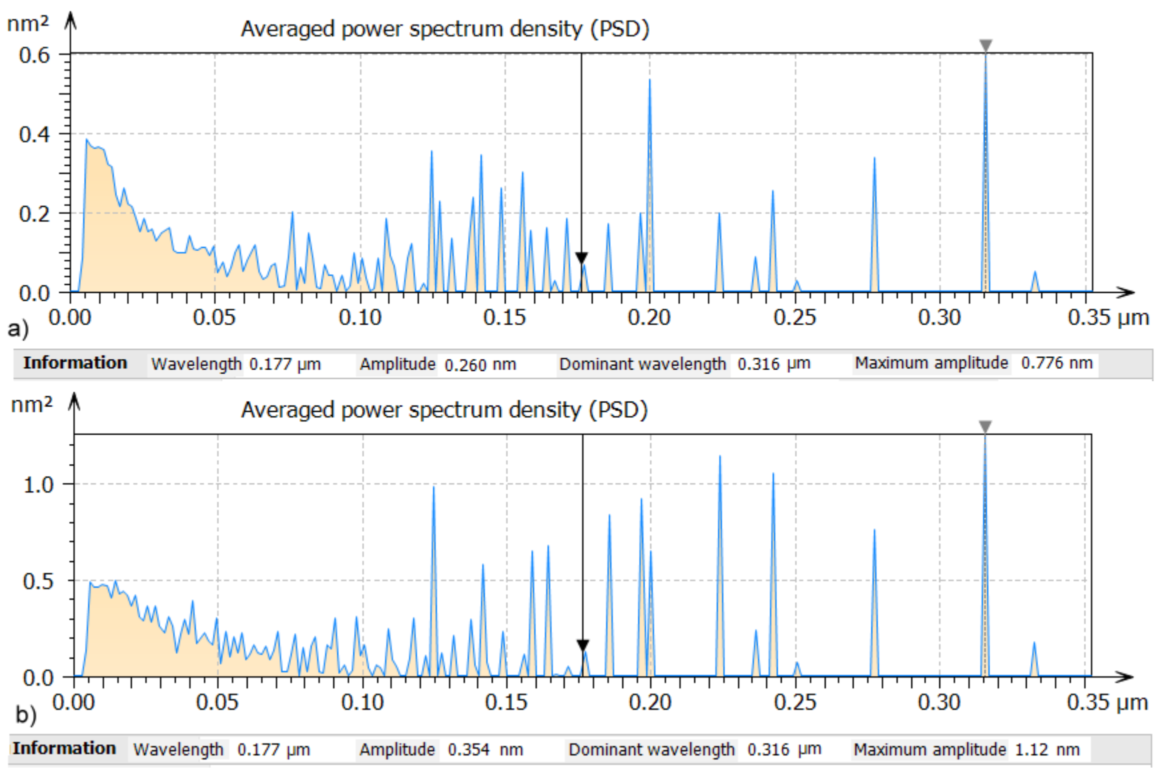

Figure 6. The representation of averaged PSD of surface textures for: a) group I; b) group II.

For both samples, wavelength and dominant wavelength have the same values, whilst amplitude and maximum amplitude is greater for group II.
Graphical representations of the slices of the analyzed samples are presented in figure 7.

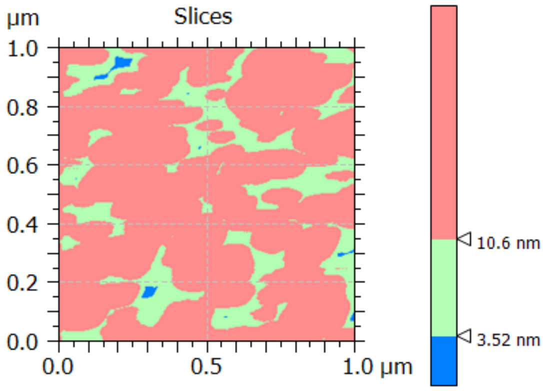

Parameters	Unit	■ (blue)	□ (green)
Projected area	%	0.494	19.4
Volume of void	%	0.152	5.94
Volume of material	%	99.8	94.1
Volume of void	nm³/µm²	5352	420088
Volume of material	nm³/µm²	3510760	6651245
Mean thickness of void	nm	0.00535	0.420
Mean thickness of material	nm	3.51	6.65

a)

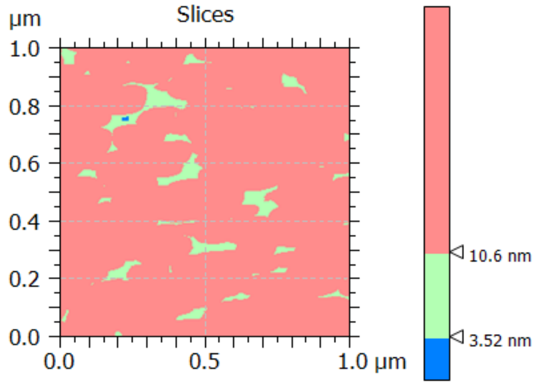

Parameters	Unit	■ (blue)	□ (green)
Projected area	%	0.0305	5.25
Volume of void	%	0.0119	1.18
Volume of material	%	100	98.8
Volume of void	nm³/µm²	420	83519
Volume of material	nm³/µm²	3515726	6987786
Mean thickness of void	nm	0.00042	0.0835
Mean thickness of material	nm	3.52	6.99

b)

Figure 7. The slices for: a) group I; b) group II.

It can be noted that there are significant differences between the values of the two slices expressed in all parameters: volume of void, volume of material, mean thickness of void and mean thickness of material.
The Sk parameters of the analyzed samples are computed in Table 2.

Table 2. Sk parameters of analyzed samples.

Samples	Sk [nm]	Spk [nm]	Svk [nm]	Smr1 [%]	Smr2 [%]	Sa1 [$nm^3/\mu m^2$]	Sa2 [$nm^3/\mu m^2$]
Group I	12	3.74	3.57	10.9	92.9	204393	127503
Group II	12.7	4.27	3.71	9.93	92.2	211901	145184

The Sk values of following parameters of group II (Sk, Spk, Svk, Sa1 and Sa2) are greater than the corresponding values of group I, whilst parameters Smr1 and Smr2 are greater for group I than group II.
Graphs of the contour lines (imaginary lines with points with the same elevation) and photo simulation of the surface microtexture are presented in figure 8.

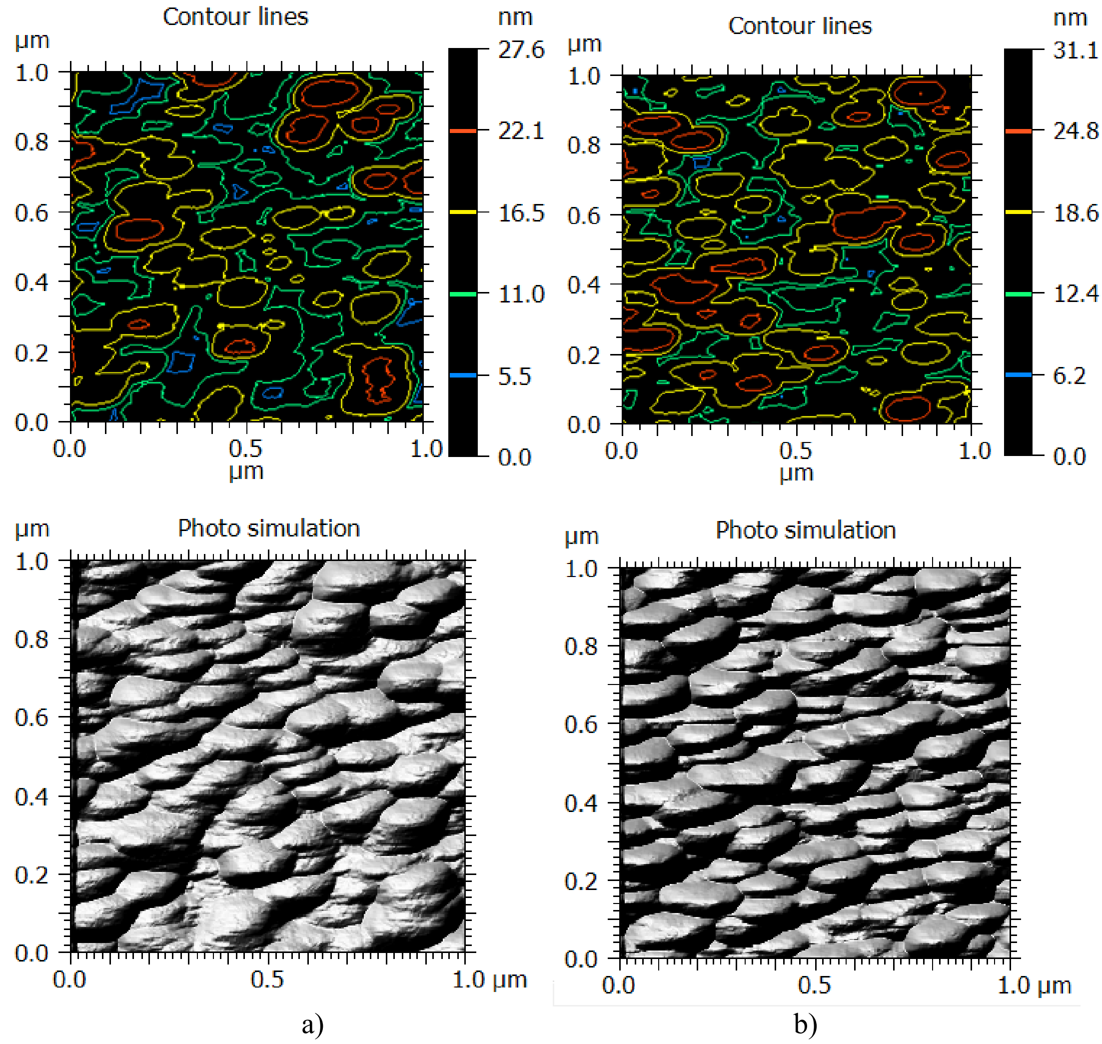

Figure 8. The graphical representation of the contour lines and photo simulation of the surface for: a) group I; b) group II.

These contours appear on associated topographic micro scale maps as colour lines and give sufficient and accurate details to facilitate reading them. Also, this comprehensive information highlights individual surface features.

These results demonstrate the applicability of the AFM system and are essential for deciphering the complexity of micromorphology of samples and for mapping their topography.

The results of the numerical calculations suggested that the surface of group I has the lowest values for fractal dimension (D = 2.28 ± 0.01) and root mean square height (Sq = 4.40 ± 0.1 nm); while the highest values for fractal dimension (D = 2.31 ± 0.01) and root mean square height (Sq = 4.67 ± 0.1 nm) were found in group II. On the other hand, the PSD highlights new information about the surface micromorphology including fractal and superstructure contributions.

4. Conclusion

In our work it is shown an advanced analysis of Cu/Fe NPs thin films fabricated by a DC magnetron sputtering technique with two controlled thicknesses 55 nm and 70 nm of Fe over layer.

The micromorphology patterns of the samples were analyzed using AFM data with a high-resolution using MountainsMap Premium software according with the standard ISO 25178-2:2012. Also, based on the quantitative tests the morphological changes of samples were examined, and we concluded that in the engineering design of Cu/Fe NPs thin films, synthesized by DC magnetron technique, this approach has several advantages over other methods to identify sets of topography parameters.

AFM platform and MountainsMap Premium software applied highlighted the multiparametric characterization capabilities and provided new perspectives in the detection of surface 3-D morphology of Cu/Fe NPs thin films.

References

[1] Laurent S, Forge D, Port M, Roch A, Robic C, Vander Elst L and Muller R N, Magnetic iron oxide nanoparticles: synthesis, stabilization, vectorization, physicochemical characterizations, and biological applications, Chem. Rev., 110, 2010. DOI: 10.1021/cr900197g.
[2] Jeevanandam J, Barhoum A, Chan Y S, Dufresne A and Danquah M K, Review on nanoparticles and nanostructured materials: history, sources, toxicity and regulations, Beilstein J Nanotechnol., 9: 1050-1074, 2018. DOI: 10.3762/bjnano.9.98.
[3] Moradian R, Ghaderi A and Elahi S M, Synthesis of Cu/Fe bilayers: micro structure and optical properties, J Mater Sci: Mater Electron, 2016. DOI 10.1007/s10854-016-4793-x.
[4] Stach S, Garczyk Z, Ţălu Ş, Solaymani S, Ghaderi A, Moradian R, Nezafat N, Elahi S M and Gholamali H, Stereometric parameters of the Cu/Fe NPs thin films, J. Phys. Chem. C 119 (31): 17887e17898, 2015. DOI: 10.1021/acs.jpcc.5b04676.
[5] Ţălu Ş, Stach S, Solaymani S, Moradian R, Ghaderi A, Hantehzadeh M R, Elahi S M, Garczyk Ż and Izadyar S, Multifractal spectra of atomic force microscope images of Cu/Fe Nanoparticles based films thickness. J Electroanal. Chem., 749: 31-41, 2015. DOI: 10.1016/j.jelechem.2015.04.009.
[6] Ţălu Ş 2015 *Micro and nanoscale characterization of three dimensional surfaces. Basics and applications* (Cluj-Napoca, Romania: Napoca Star Publishing House).
[7] Ţălu Ş, Stach S, Valedbagi S, Elahi S M and Bavadi R, Surface morphology of titanium nitride thin films synthesised by DC reactive magnetron sputtering, Mater Sci-Poland, 33(1): 137-143, 2015. DOI: 10.1515/msp-2015-0010.
[8] Stach S, Dallaeva D, Ţălu Ş, Kaspar P, Tománek P, Giovanzana S and Grmela L, Morphological features in aluminum nitride epilayers prepared by magnetron sputtering, Mater Sci-Poland, 33(1): 175-184, 2015. DOI: 10.1515/msp-2015-0036.
[9] Ţălu Ş, Stach S, Valedbagi S, Bavadi R, Elahi S M and Ţălu M, Multifractal characteristics of titanium nitride thin films, Mater Sci-Poland, 33(1): 541-548, 2015. DOI: 10.1515/msp-2015-0086.
[10] Arman A, Ţălu Ş, Luna C, Ahmadpourian A, Naseri M and Molamohammadi M, Micromorphology characterization of copper thin films by AFM and fractal analysis, J. Mater. Sci. Mater. Electron., 26: 9630–9639, 2015. DOI: 10.1007/s10854-015-3628-5.
[11] Shikhgasan R, Ţălu Ş, Dinara S, Sebastian S and Guseyn R, Epitaxy of silicon carbide on silicon: Micromorphological analysis of growth surface evolution, Superlattices Microstruct. 86: 395-402, 2015. DOI: 10.1016/j.spmi.2015.08.007.
[12] Ţălu Ş, Solaymani S, Bramowicz M, Kulesza S, Ghaderi A, Shahpouri S and Elahi S M, Effect of electric field direction and substrate roughness on three-dimensional self-assembly growth of copper oxide nanowires, J. Mater. Sci. Mater. Electron., 27(9): 9272-9277, 2016. DOI: 10.1007/s10854-016-4965-8.
[13] Sobola D, Ţălu Ş, Solaymani S and Grmela L, Influence of scanning rate on quality of AFM image: Study of surface statistical metrics. Microsc. Res. Tech., 80(12): 1328-1336, 2017. DOI: 10.1002/jemt.22945.
[14] Ţălu Ş, Bramowicz M, Kulesza S, Dalouji V, Solaymani S and Valedbagi S, Fractal features of carbon–nickel composite thin films, Microsc. Res. Tech., 79(12): 1208-1213, 2016. DOI: 10.1002/jemt.22779.
[15] Ţălu Ş, Stach S, Mendez A, Trejo G and Ţălu M., Multifractal characterization of nanostructure surfaces of electrodeposited Ni-P Coatings, J. Electrochem. Soc., 161: D44–D47, 2013. DOI:10.1149/2.039401jes.
[16] Yadav R P, Kumar M, Mittal A K and Pandey A C, Fractal and multifractal characteristics of swift heavy ion induced self-affine nanostructured BaF_2 thin film surfaces, Chaos, 25(8): 083115, 2015.

[17] Ţălu Ş, Marković Z, Stach S, Marković B T and Ţălu M, Multifractal characterization of single wall carbon nanotube thin films surface upon exposure to optical parametric oscillator laser irradiation, Appl Surf Sci, 289: 97-106, 2014. DOI: 10.1016/j.apsusc.2013.10.114.

[18] Ţălu Ş, Morozov I A and Yadav R P, Multifractal analysis of sputtered indium tin oxide thin film surfaces, Appl Surf Sci., 484: 892-898, 2019. DOI: 10.1016/j.apsusc.2019.04.170.

[19] Senthilkumar M, Sahoo N K, Thakur S and Tokas R, Characterization of microroughness parameters in gadolinium oxide thin films: A study based on extended power spectral density analyses, Appl Surf Sci., 81(5), 2005. DOI: 10.1016/j.apsusc.2005.02.122.

[20] Mwema F M, Akinlabi E and Oladijo P 2019 The use of Power Spectrum Density for surface characterization of thin films, *Photoenergy and Thin Film Materials.* (John Wiley & Sons). DOI: 10.1002/9781119580546.ch9.

[21] Gong Y, Misture S T, Gao P and Mellott N P, Surface roughness measurements using power spectrum density analysis with enhanced spatial correlation length, J. Phys. Chem. C, 120(39): 22358-22364, 2016. DOI: 10.1021/acs.jpcc.6b06635.

[22] Méndez A, Reyes Y, Trejo G, Stępień K and Ţălu Ş, Micromorphological characterization of zinc/silver particle composite coatings. Microsc. Res. Tech., 78(12): 1082-1089, 2015. DOI: 10.1002/jemt.22588.

[23] Zare M, Solaymani S, Shafiekhani A, Kulesza S, Ţălu Ş and Bramowicz M, Evolution of rough-surface geometry and crystalline structures of aligned TiO_2 nanotubes for photoelectrochemical water splitting. Sci Rep., 8: 1-11, article number: 10870, 2018. DOI: 10.1038/s41598-018-29247-3.

[24] Stach S, Sapota W, Ţălu Ş, Ahmadpourian A, Luna C, Ghobadi N, Arman A and Ganji M, 3D surface stereometry studies of sputtered TiN thin films obtained at different substrate temperatures. J. Mater. Sci. Mater. Electron., 28(2): 2113-2122, 2017. DOI: 10.1007/s10854-016-5774-9.

[25] Naseri N, Solaymani S, Ghaderi A, Bramowicz M, Kulesza S, Ţălu Ş, Pourreza M and Ghasemi S, Microstructure, morphology and electrochemical properties of Co nanoflake water oxidation electrocatalyst at micro- and nanoscale. RSC Advances, 7(21): 12923-12930, 2017. DOI: 10.1039/c6ra28795f.

[26] Jacobs TDB, Junge T and Pastewka L, Quantitative characterization of surface topography using spectral analysis. Surf. Topogr.: Metrol. Prop., 5(1): 013001, 2017. DOI: 10.1088/2051-672X/aa51f8.

[27] Martínez JFG, Nieto-Carvajal I, Abad J and Colchero J, Nanoscale measurement of the power spectral density of surface roughness: how to solve a difficult experimental challenge. Nanoscale Res Lett., 7(1): 174, 2012. DOI: 10.1186/1556-276X-7-174.

[28] Gavrilă R, Dinescu A and Mardare D, A power spectral density study of thin films morphology based on AFM profiling, Rom J Inf Sci Tech., 10(3): 291-300, 2007.

[29] Karana S and Mallik B, Power spectral density analysis and photoconducting behavior in copper(II) phthalocyanine nanostructured thin films. Phys. Chem. Chem. Phys., 10: 6751-6761, 2008. DOI: 10.1039/B809648A.

[30] Itoh T and Yamauchi N, Surface morphology characterization of pentacene thin film and its substrate with under-layers by power spectral density using fast Fourier transform algorithms. Appl Surf Sci., 253(14): 6196-6202, 2007. DOI: 10.1016/j.apsusc.2007.01.056.

[31] Dash P, Mallick P, Rath H, Tripathi A, Prakash J, Avasthi DK, Mazumder S, Varma S, Satyam PV and Mishraa NC, Surface roughness and power spectral density study of SHI irradiated ultra-thin gold films. Appl Surf Sci., 256(2): 558-561, 2009. DOI: 10.1016/j.apsusc.2009.08.046.

[32] Yu L, Xu J, Dong S and Kojima I, Surface morphology and growth mechanisms for sputtered amorphous silicon nitride thin films, Thin Solid Films, 516(8): 1781-1787, 2008. DOI: j.tsf.2007.07.158.

[33] MountainsMap® Premium 7.4.8872 software (Digital Surf, Besançon, France).

[34] ISO 25178-2: 2012, Geometrical product specifications (GPS) - Surface texture: Areal - Part 2: Terms, definitions and surface texture parameters.